required to assign $\Delta\phi$ in the former and Δs^2 in the latter. Since the optimum procedure for controlling either is a 'will-o'-the wisp" and can never be found, it is not surprising that independent attempts at controlling them has not yielded equivalent algorithms. The results given herein and in Ref. 7 can be immediately employed to transform a given gradient projection algorithm into the equivalent minimum norm algorithm, and vice versa. These results therefore can be used to eliminate redundancy in existing computer programs and will allow improved understanding of these often-used techniques.

References

[1] Bryson, A. E., and Ho, Y. C., *Applied Optimal Control,* Blaisdell, Waltham, Mass., 1969, pp. 222–228.

[2] Kelly, H. J., "Method of Gradients," *Optimization Techniques,* edited by G. Leitman, Academic Press, London, 1962, Chap. 6.

[3] Beskind, B. L., "An N-Dimensional Search and Optimization Procedure," Rept. SSD-TR-63-324, Dec. 6, 1963, Aerospace Corp.

[4] Glassman, B. A. et al., "A Parameter Optimization Procedure for Multi-Stage Vehicles," AAS Paper 66-111, AAS Space Flight Mechanics Specialist Conference, Univ. of Denver, July 6–8, 1966.

[5] Junkins, J. L., "On the Determination and Optimization of Powered Space Vehicle Trajectories Using Parametric Differential Correction Processes," Rept. G1793, Dec. 1969, McDonnell Douglas, Huntington Beach, Calif.

[6] Korn, G. A. and Korn, T. M., *Mathematical Handbook for Engineers and Scientists,* McGraw-Hill, New York, 1961, pp. 203–204.

[7] Junkins, J. L., "Equivalence of the Minimum Norm and Gradient Projection Constrained Optimization Techniques," AAS Paper 71-307, AAS/AIAA Astrodynamics Specialist Conference 1971, Ft. Lauderdale, Fla., Aug. 17–19, 1971.

Flow Pattern of Two Impinging Circular Jets

MICHEL A. SAAD* AND GENE J. ANTONIDES†

University of Santa Clara, Santa Clara, Calif.

THIS Note describes a method to determine the flow pattern resulting from the impingement of two circular liquid streams. Using finite-difference techniques, values of the stream function are calculated and the velocity and pressure distributions along the impingement surface are obtained.

Figure 1 shows two circular jets impinging on each other. The centerlines of the two jets coincide so that the flow is axially symmetric. The flow is assumed to be inviscid, incompressible and irrotational, and no mixing of the two streams occurs. Because of symmetry, the stream function, ψ, can be defined by

$$u = (1/r)\,\partial\psi/\partial z \tag{1}$$

and

$$w = -(1/r)\,\partial\psi/\partial r \tag{2}$$

where r is the radial coordinate, z is the axial coordinate, and u and w are the radial and axial components of fluid velocity, respectively. The equation of irrotationality in axisymmetric flow is

$$\partial u/\partial z - \partial w/\partial r = 0 \tag{3}$$

Received October 29, 1971; revision received January 24, 1972. Research sponsored by Air Force Office of Scientific Research under Grant AFOSR-68-1478C.

Index category: Jets, Wakes, and Viscid-Inviscid Flow Interactions.

* Professor of Mechanical Engineering. Member AIAA.

† Graduate Student. Member AIAA.

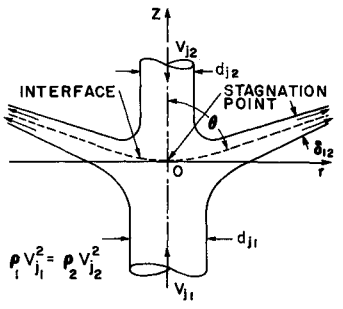

Fig. 1 Impingement of unequal, opposite, circular jets.

Substituting Eqs. (1) and (2) into Eq. (3) yields the following equation for the stream function:

$$\partial^2\psi/\partial r^2 + \partial^2\psi/\partial z^2 - (1/r)\,\partial\psi/\partial r = 0 \tag{4}$$

A necessary condition for a meaningful problem is that the stagnation pressures of the two jets be equal. Otherwise, the jet of higher stagnation pressure would drive the other jet back to its source. The stagnation pressure is given by

$$p_s = p_a + \rho V_j^2/2g \tag{5}$$

where p_s is the stagnation pressure, p_a is the ambient pressure, ρ is the fluid density, and V_j is the upstream jet velocity. It is assumed that the two jets have equal density and initial velocity, thereby satisfying the requirement for equal stagnation pressures. The velocity and pressure distributions at the interface are found from the steady flow Bernoulli's equation

$$p_s = p + \rho u^2/2g \tag{6}$$

The static pressure p must be continuous across the impingement surface, and therefore the velocity must also be continuous.

The boundary conditions applied to the model are as follows:[1] 1) The fluid velocity V_j along the jets' free surface is constant and in view of Eqs. (1) and (2), the gradient of ψ at the free surface and normal to it, $\partial\psi/\partial n$, is equal to $V_j r$. 2) The stream function ψ along the centerline of each jet and on the impingement surface is a constant and is set equal to zero. 3) It is assumed that the fluid velocity V_j across the boundaries of the incoming and outgoing flow is constant. Therefore, the stream function ψ at the upstream boundary is equal to $\frac{1}{2}V_j r^2$, and the stream function at the outgoing boundary is equal to $V_j rz$ $(\sin\theta)$, where z is the axial distance from the impingement surface and θ is the angle between the jets' axis and the final flow direction of the outgoing flow. 4) The stream function ψ on the free surface is constant and, according to conditions 2 and 3, is equal to $\frac{1}{2}V_j r_j^2$, where r_j is the upstream jet radius.

The boundary for the incoming flow is established at an axial distance $3r_j$ from the stagnation point. The boundary for the outgoing fluid sheet is at a radial distance $4r_j$ from the stagnation point. These boundaries are based on experimental results[2] and represent the locations where the jet flow begins to deviate due to impingement. Since the downstream boundary is chosen at $4r_j$, then ψ on this boundary is $4V_j r_j z\,(\sin\theta)$.

Method of Solution

By assuming the surface contours of the two jets and the contour of the impingement surface, and a set of boundary conditions on these surfaces, a solution to Eq. (4) can be obtained for each jet. A second boundary condition on each of the assumed surfaces is then applied to determine whether the assumed contours are correct. The solution for the jet flow is obtained when the jets' boundaries satisfy both sets of boundary conditions. The first boundary condition at each free surface is that ψ is constant and equal to $\frac{1}{2}V_j r_j^2$. The second boundary condition is $\partial\psi/\partial n = V_j r$. At the impingement surface, the first and second boundary conditions are, respectively, $\psi = 0$ and the pressure distribution of the two jets match. Solutions are obtained for each jet separately, assuming an interface contour and calculating the free surface contour which is correct for that interface. If the interface pressure distributions do not match, the interface contour is modified and the procedure is repeated.

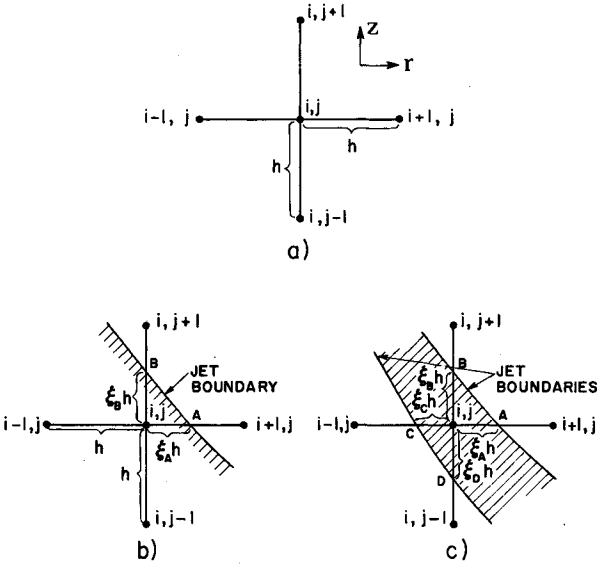

Fig. 2 Node notation a) for an interior point, b) with jet boundary intercepting two mesh lines, and c) with two jet boundaries intercepting all four mesh lines.

In order to obtain the results in a nondimensional form, the stream function was set equal to 1 on the free surface and the jet radius was assigned the value 1. Then from the equation for the stream function along the upstream boundary, it is found that $V_j = 2$.

In the finite-difference method, a square grid of spacing h is superimposed on an axial plane with the origin placed arbitrarily at the stagnation point. Finite-difference approximations of the partial derivatives in Eq. (4) are formulated to calculate the stream function, ψ, at the intersections of the grid lines. A successive over-relaxation method is employed.

The finite-difference approximations of the partial derivatives are

$$\partial\psi_{i,j}/\partial r \simeq (\psi_{i+1,j}-\psi_{i-1,j})/2h \tag{7}$$

$$\partial^2\psi_{i,j}/\partial r^2 \simeq (\psi_{i+1,j}-2\psi_{i,j}+\psi_{i-1,j})/h^2 \tag{8}$$

and

$$\partial^2\psi_{i,j}/\partial z^2 \simeq (\psi_{i,j+1}-2\psi_{i,j}+\psi_{i,j-1})/h^2 \tag{9}$$

where the i, j subscripts refer to mesh points as shown in Fig. 2a. Upon substitution into Eq. (4) one obtains

$$\psi_{i,j} = \tfrac{1}{4}[(1-h/2r)\psi_{i+1,j}+(1+h/2r)\psi_{i-1,j}+\psi_{i,j+1}+\psi_{i,j-1}] \tag{10}$$

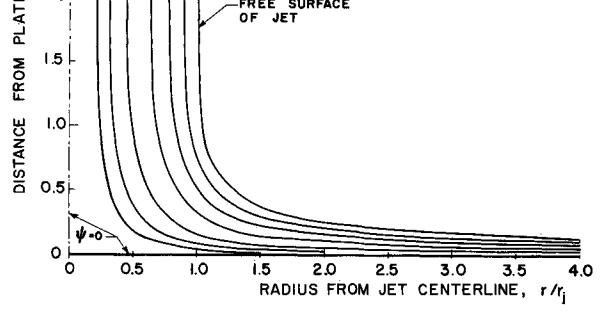

Fig. 3 Flow streamlines in circular jet impinging on a perpendicular surface.

Denoting two successive iterations by n and $n+1$, then:

$$\psi_{i,j}^{(n+1)} = (1-\omega)\psi_{i,j}^{(n)}+(\omega/4)[(1-h/2r)\psi_{i+1,j}+(1+h/2r)\psi_{i-1,j}+\psi_{i,j+1}+\psi_{i,j-1}] \tag{11}$$

where ω is the relaxation parameter.

Special finite-difference equations are required where one or more grid lines is intercepted by a boundary of the jet as shown in Figs. 2b and 2c. When all four mesh lines are intercepted, the partial derivatives are approximated by

$$\frac{\partial\psi_{i,j}}{\partial r} \simeq \frac{1}{h}\left[\frac{\xi_C}{\xi_A(\xi_A+\xi_C)}\psi_A - \frac{\xi_A}{\xi_C(\xi_A+\xi_C)}\psi_C + \frac{\xi_A-\xi_C}{\xi_A\xi_C}\psi_{i,j}\right] \tag{12}$$

$$\frac{\partial^2\psi_{i,j}}{\partial r^2} \simeq \frac{2}{h^2}\left[\frac{1}{\xi_A(\xi_A+\xi_C)}\psi_A + \frac{1}{\xi_C(\xi_A+\xi_C)}\psi_C - \frac{1}{\xi_A\xi_C}\psi_{i,j}\right] \tag{13}$$

$$\frac{\partial^2\psi_{i,j}}{\partial z^2} \simeq \frac{2}{h^2}\left[\frac{1}{\xi_B(\xi_B+\xi_D)}\psi_B + \frac{1}{\xi_D(\xi_B+\xi_D)}\psi_D - \frac{1}{\xi_B\xi_D}\psi_{i,j}\right] \tag{14}$$

and ψ is calculated from

$$\psi_{i,j}^{(n+1)} = (1-\omega)\psi_{i,j}^{(n)}+\omega\left[\frac{2-(h/r)\xi_C}{\xi_A(\xi_A+\xi_C)}\psi_A + \frac{2}{\xi_B(\xi_B+\xi_D)}\psi_B + \frac{2+(h/r)\xi_A}{\xi_C(\xi_A+\xi_C)}\psi_C + \frac{2}{\xi_D(\xi_B+\xi_D)}\psi_D\right] \Big/ \left[\frac{2+(h/r)(\xi_A-\xi_C)}{\xi_A\xi_D} + \frac{2}{\xi_B\xi_D}\right] \tag{15}$$

The gradient $\partial\psi/\partial r$ at the free surface of the jet, used in determining $\partial\psi/\partial n$, requires an "off-center" approximation which is

$$\frac{\partial\psi_A}{\partial r} \simeq \left[\frac{1}{\xi_A}\left(2+\frac{1}{\xi_A}\right)\psi_A - \left(1+\frac{1}{\xi_A}\right)^2\psi_{i-1,j} + \psi_{i-2,j}\right] \Big/ h\left(1+\frac{1}{\xi_A}\right) \tag{16}$$

The calculations were performed on an IBM 1130 digital computer.

Results

When the two impinging jets are equal in diameter, velocity and dynamic pressure, the impingement surface is a plane perpendicular to the axis of the jets. Thus, the interface is known, and only the free surface is assumed and modified to determine the flow pattern. The results are shown in Fig. 3 where the flow streamlines including the free surface contour are given. The velocity and static pressure distributions are shown in Fig. 4.

Figure 5 presents the calculated streamlines of two unequal jets, and the corresponding velocity and pressure distributions at the interface are shown in Fig. 4, where r_j is the larger jet radius.

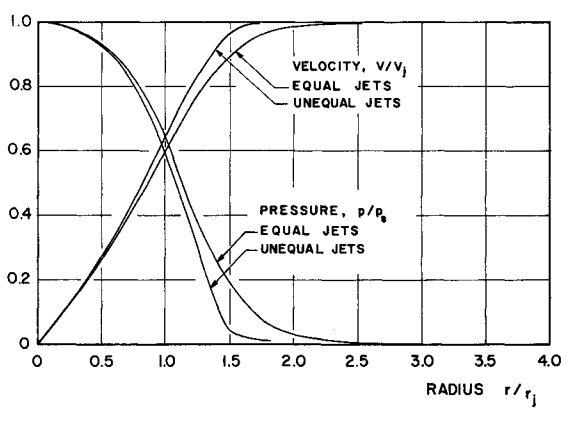

Fig. 4 Velocity and pressure distributions at the interface of impinging circular jets.

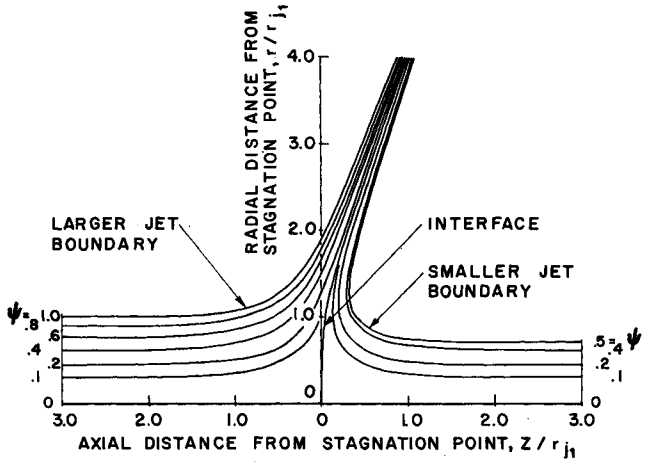

Fig. 5 Flow streamlines in unequal, opposite, circular jets.

References

[1] Birkhoff, G. and Zarantonello, E. H., *Jets, Wakes and Cavities*, Academic Press, New York, 1957.

[2] Schach, W., "Umlenkung eines kreisförmigen Flussigkeitsstrahles an einer ebenen Platte senkrecht zur Stromungrictung," *Inginieur-Archiv*, Vol. 6, 1935, pp. 51–58.

Elastic Behavior of Multilayered Bidirectional Composites

N. J. PAGANO*

Air Force Materials Laboratory, Dayton, Ohio

AND

SHARON J. HATFIELD†

Aeronautical Systems Division, Dayton, Ohio

SEVERAL recent papers[1-5] have addressed the problem of defining the exact (elastic) response of composite laminates under static bending. However, all of these studies have treated laminates consisting of only a few layers, while in practical applications, composite structures may consist of many layers, in some cases, 100 or more. It is therefore appropriate that we consider the response of multi-ply laminates with a view toward examining the generality of previous conclusions regarding the range of validity of the approximate theory normally used in the analysis of these bodies, namely, classical laminated plate theory (CPT).[6]

Previous investigations[1-5] have shown that the exact solution for a particular composite laminate converges to the respective CPT solution as the aspect ratio becomes very large. Furthermore, the exact solution for the stress field generally converges more rapidly than that for deflection. In particular, a good estimate for the maximum normal stress is given by CPT for aspect ratios as low as 10, while for highly anisotropic materials, the error in the CPT deflection estimate can be appreciable for aspect ratios as high as 30. The objective of the present work is to examine these trends for laminates composed of many layers. Specifically, we treat the boundary value problem discussed in Ref. 2 for square bidirectional laminates of edge dimension a and

Received October 29, 1971; revision received January 26, 1972.

Index category: Structural Composite Materials (Including Coatings).

* Materials Research Engineer, Nonmetallic Materials Division.

† Mathematician, 4950th Test Wing (Technical), VNCP.

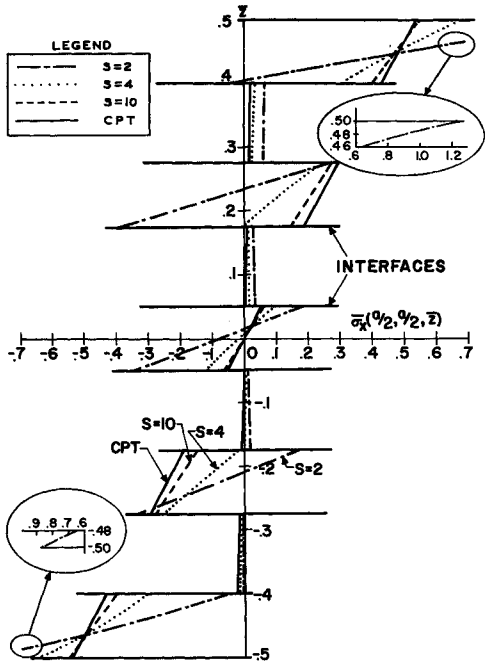

Fig. 1 Normal stress distribution.

thickness h consisting of 3, 5, 7, and 9 layers under the surface loading

$$q_0 = \sigma \sin(\pi x/a) \sin(\pi y/a) \quad (0 \leqq x \leqq a,\ 0 \leqq y \leqq a,\ -h/2 \leqq z \leqq h/2) \tag{1}$$

where σ is a constant. Each layer is a unidirectional fiber reinforced composite possessing the following engineering constants:

$$E_L = 25 \times 10^6 \text{ psi}, \quad E_T = 10^6 \text{ psi}, \quad G_{LT} = 0.5 \times 10^6 \text{ psi}$$
$$G_{TT} = 0.2 \times 10^6 \text{ psi}, \quad \nu_{LT} = \nu_{TT} = 0.25 \tag{2}$$

where L signifies the fiber direction, T the transverse direction, ν_{LT} is the major Poisson ratio, and the material is assumed to be square-symmetric. All laminates considered are symmetric with respect to the central plane, with fiber orientations alternating

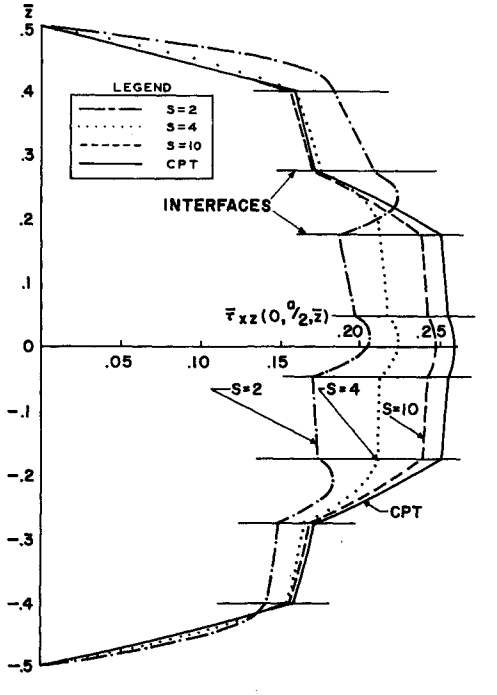

Fig. 2 Shear stress distribution.